Astron. Astrophys. 326, 1135–1142 (1997)

ASTRONOMY
AND
ASTROPHYSICS

Zeeman-Doppler imaging of active stars

V. Sensitivity of maximum entropy magnetic maps to field orientation

J.-F. Donati[1] **and S.F. Brown**[2,⋆]

[1] Laboratoire d'Astrophysique, Observatoire Midi-Pyrénées, F-31400 Toulouse, France (donati@obs-mip.fr)
[2] School of Mathematics and Statistics, The University of Sydney, Sydney 2006, Australia (sbrown@tip.csiro.au)

Received 12 December 1996 / Accepted 13 May 1997

Abstract. In 1989, Semel proposed a new technique (dubbed Zeeman-Doppler imaging or ZDI) for measuring and mapping magnetic fields at the surface of cool active stars from sets of rotationally modulated circularly polarised (Stokes V) profiles of spectral lines. Two years later, an automatic tool (based on maximum entropy image reconstruction techniques) was developed and checked on a few test cases (Brown et al. 1991). In particular, this paper established that surface magnetic distributions consisting in circular regions of radially oriented field can be very well recovered with ZDI.

In the present paper, we show new simulations demonstrating that ZDI is good at reconstructing the *field orientation* within magnetic regions. In particular, it can always unambiguously identify azimuthal from radial/meridional field features (where radial, azimuthal and meridional refer to the three vector field components in spherical geometry). For high latitude magnetic spots, all three field components can be recovered. For low latitude regions however, ZDI (from circular polarimetry alone) suffers some crosstalk from radial to meridional field components (or vice versa), especially at low stellar inclination angles.

Key words: stars: magnetic fields – stars: imaging – stars: activity – line: profiles – polarization – methods: observational

1. Introduction

Activity in most cool stars is found to be essentially similar to that of the Sun (with different strengths and variability timescales though) and it thus also attributed to dynamo mechanisms operating in (or at least at the base of) their convective envelope. As solar observations are much more detailed than stellar observations, they represent most of what we know to date about how stellar dynamos operate. However, despite several decades of efforts, theoreticians have still not been able to converge onto an adequate, self-consistent MHD model of the solar convective zone that reproduces quantitatively all relevant observations at the same time (Brandenburg & Tuominen 1992). Even if much poorer in terms of spatial resolution, stellar observations represent a very rich potential source of information as they can tell us how dynamo processes depend on fundamental stellar parameters such as mass, age, photospheric temperature and rotational velocity (Baliunas et al. 1995). A new method, called Zeeman-Doppler imaging or ZDI (Semel 1989), should in particular allow us to access some crucial piece of information about stellar dynamos – the detailed topology of the stellar surface magnetic structure as well as its variation throughout a complete activity cycle – information that has remained out of reach of all existing observational techniques to date.

This new method is very similar to Doppler imaging and aims at reconstructing stellar surface magnetic topologies of rapid rotators from sets of rotationally modulated circularly polarised (Stokes V) profiles of photospheric spectral lines. In 1991, Brown et al. developed a computer code (based on maximum entropy image reconstruction techniques) that can automatically reconstruct a magnetic stellar image from spectropolarimetric data sets, thus placing ZDI on a similar footing to conventional Doppler imaging. In this first paper, the authors carried out a series of simulations, proving that spot distributions could be successfully recovered from sets of rotationally modulated Stokes V (circular polarisation) profiles. However, these simulations were restricted to radial field distributions only, reconstructed under a radial field assumption. Although it seemed like a reasonable hypothesis at that time, it no longer appears to be appropriate, especially when referring to more recent results obtained on cool active stars (Donati at al. 1992) where regions of mainly azimuthal field were detected.

In this paper, we carry out a new series of simulations pointing out the capabilities (and potential problems) of ZDI in a much more general context. We still restrict ourselves to Stokes V data sets (linear polarisation line profiles are not available yet) but now consider more complex field geometries, involv-

Send offprint requests to: J.-F. Donati

⋆ On leave at Observatoire de Paris-Meudon in 1993. Now at CSIRO Telecommunications and Industrial Physics.

ing magnetic spots with various vector field orientations. We use both analytical arguments and simulated spectra from various kind of elementary field configurations (forward problem) to illustrate how ZDI is expected to behave. We confirm the expected behaviour by testing the complete inversion procedure with simulated spectra. Details on the maximum entropy inversion code (described extensively in Brown et al. 1991) will not be repeated here and are supposed to be known to the reader.

2. Properties of Stokes V profiles

With dynamic Stokes V spectra of single spot magnetic topologies (see next section), we can empirically study how circular polarisation profiles respond to various simple field geometries. In other words, we want to study the response matrix (i.e. the locally linearised operator that translates a given magnetic image into the corresponding Stokes V data set) and estimate how well the associated inverse problem is conditioned.

The information a dynamic Stokes V spectrum can yield on a magnetic spot is double. Firstly, the radial velocity excursion of a line distortion throughout a rotationally broadened profile tracks the location of the parent spot, just as in conventional Doppler imaging. We thus expect spot locations to be well recovered, as already demonstrated for radial field features in Brown et al. (1991). The information on field orientation comes from the fact that circular polarisation is sensitive to the *line of sight component* of the magnetic vector; different field orientations will thus modulate the overall *amplitude and/or shape* of the Stokes V signature differently. In the following, we will study the characteristic Zeeman signatures of different field orientation and the extent to which the inversion code can mistake one field orientation for another. The three basic field orientations we consider in this paper (radial, azimuthal and meridional) correspond to the three vector field components in spherical geometry, known to be key field directions for dynamo mechanisms.

2.1. The line profile model

For our simulations, we assume that the local profile *including macroturbulence and instrumental broadening* is Gaussian. In addition to being the simplest possible model, this description has the strong advantage of being fairly close to reality when one is dealing with profiles of "average lines" (obtained from "Least-Squares Deconvolution" of over 2,000 individual spectral features, see Donati et al. 1997; Donati & Cameron 1997), something one *has* to do anyway for ZDI to decrease the relative noise level in Stokes V profiles. This Gaussian "average local profile" features (in absence of magnetic fields) a central depression of 50% of the continuum level and a full width at half maximum of 10 $\mathrm{km\,s^{-1}}$ (equivalent to a global Doppler width of 6 $\mathrm{km\,s^{-1}}$). We further assume that this local profile is a normal Zeeman triplet centred on 550 nm with a magnetic sensitivity (i.e. Landé factor) of 1.5. The continuum limb-darkening constant is set to 0.75. This is similar to what we observe for the photosphere of cool active stars (e.g. Donati & Cameron 1997).

For a field strength of 500 G, the Zeeman splitting v_{B} (equal to 0.4 $\mathrm{km\,s^{-1}}$) is small compared to the Doppler width v_{D} of the *true* instrinsic profile (i.e. prior to macroturbulence and instrumental broadening), typically equal to $v_{\mathrm{D}} = 2\ \mathrm{km\,s^{-1}}$ for the cool stars we are interested in. In this context, the weak field regime ($v_{\mathrm{B}}/v_{\mathrm{D}} \leq 0.5$) holds, implying that Stokes V signatures of infinitesimal stellar surface regions (called image pixels in the following) are proportional to the derivative of the Gaussian local profile and depend *linearly* on the local magnetic field vector **B**. The response matrix is therefore independent on **B** up to field strengths of about 1.2 kG. Above this threshold, the weak field approximation is in principle no longer valid; however, we actually observe (on very slowly rotating moderately magnetised Ap stars like γ Equ, see Donati & Cameron 1997) that it is still perfectly adequate to describe (at a spectral resolution of about 50,000) average local Stokes V profiles up to field strengths of at least 5 kG. We can thus conclude that, for our particular purpose, Stokes V signatures of individual image pixels are only modulated in *amplitude* and spectral location, while their *shape* should remain constant.

Note that magnetic fields in solar-type stars are likely to be stronger than 500 G. However, stellar surface magnetic regions are often associated with a local atmospheric temperature deficit of 500 K to 1,000 K (and possibly more), as demonstrated recently by Donati et al. (1997). Moreover, observations show that this temperature difference affects mainly the global strength of the average local profile (estimated from Least-Squares Deconvolved spectra of slowly rotating standard stars with different spectral types, Donati & Cameron 1997), whose *shape* (and in particular its full width at half maximum) remains almost constant with temperature (within about 5% at a spectral resolution of 50,000). The overall effect of this spot to photosphere temperature contrast is thus to decrease the *amplitude* of the associated Zeeman signature, *just as a lower magnetic field would do* (as long as the weak field linear regime holds). Therefore, what polarisation and ZDI are altogether sensitive to is local magnetic *flux* (weighted by inhomogeneities in atmospheric brightness and intrinsic profile equivalent width), possibly up to five times smaller than actual field strength. To make things simpler, we thus consider in this study magnetic regions at photospheric temperature with unit filling factors and 500 G fields, totally equivalent (in terms of Stokes V signatures) to 2 kG field spots with 50% filling factors and 50% temperature-induced signal dilution (typical of what we expect on very active cool stars). Note in particular that this simplification does not restrict at all the validity of our conclusions.

2.2. *Effects of field orientation on Stokes V signatures*

Let us first consider polarisation signatures produced by a given image pixel. The first kind of *amplitude modulation* such polarisation signatures are subject to is of course limb darkening. As it affects all types of Zeeman signatures (i.e. from all three basic vector field orientations) the same way, we can ignore it in the following argument. The amplitude of the polarisation signal then depends on two terms. The first one is constant with rotational phase ϕ and corresponds to the contribution of the local vector magnetic field projected onto the rotation axis. The second term fluctuates sinusoidally with ϕ and represents the contribution of the field component perpendicular to the rotation axis.

For an azimuthal field (always perpendicular to the rotation axis), the constant term is equal to zero while the second term is proportional to $\sin 2\pi(\phi - \phi_s)$ (where ϕ_s denotes the phase at which the image pixel we consider gets closest to stellar disc centre). In contrast, radial/meridional fields generate non zero constant and oscillating terms, the latter being proportional to $\cos 2\pi(\phi - \phi_s)$. The first major difference is thus that the amplitude modulation is symmetric in ϕ (with respect to ϕ_s) for a radial/meridional vector field, while it is *antisymmetric* for an azimuthal vector field. We thus expect very different Zeeman signatures for azimuthal and radial/meridional field vectors, and therefore very little crosstalk from the inversion code between these two orientations.

For radial and meridional field vectors, the problem is more complex. Although the amplitude modulation of circular polarisation signatures is symmetric in ϕ for both field orientations, a closer look reveals that it usually differs (at least slightly) in overall shape. From straightforward arithmetic in spherical coordinates, we obtain the following equations for the amplitude modulation of Stokes signatures V_r and V_m (corresponding to radial and meridional field respectively):

$$\left\{ \begin{array}{lll} V_r(\phi) & \propto & \cos i \ \sin l + \sin i \ \cos l \ \cos 2\pi(\phi - \phi_s) \\ V_m(\phi) & \propto & \cos i \ \cos l - \sin i \ \sin l \ \cos 2\pi(\phi - \phi_s) \end{array} \right. \quad (1)$$

where l denotes the latitude of the associated image pixel and i the angle of the rotation axis to the line of sight. In particular, we see that, whenever the first (constant) terms have the same sign, the second (oscillating) terms have opposite signs (or vice versa). However, this difference may be small in some cases. For instance, in the two degenerate cases $i = 0°$ and $i = 90°$ (where the star is seen exactly pole-on and equator-on respectively), V_r and V_m are both constant or purely sinusoidal, and thus cannot be differentiated by an inversion procedure. More problematic is the case when the sampling of V_r and V_m is sparse and/or available on no more than a narrow range of rotational phases about ϕ_s, i.e. for low latitude field regions (with $l < i$) and especially when limb darkening is severe. In such conditions, the cosine term is indeed weakly variable and Eqs. 1 reduce to:

$$\left\{ \begin{array}{lllll} V_r(\phi) & \simeq & \text{constant} & \propto & \sin(i + l) \\ V_m(\phi) & \simeq & \text{constant} & \propto & \cos(i + l) \end{array} \right. \quad (2)$$

At this point, the entropy criterion comes into action (to solve the response matrix degeneracy) and select the field orientation with the strongest sensitivity in order to generate the spot with the weakest contrast. We thus expect to obtain some crosstalk for low latitude spots ($l < i$), from radial to meridional field components mainly if $\cos(i + l) > \sin(i + l)$ (i.e. for $i \leq 30°$), from meridional to radial field components mainly if $\sin(i+l) > \cos(i+l)$ (i.e. for $i \geq 50°$), or both in between. Note finally that, although more features are affected at *high* inclination angles (the $l < i$ latitude span increases with i), crosstalk problems tend to be worse for *low* axial inclinations (i.e. when the coefficient of the cosine term is smallest).

3. Dynamic spectra: the forward approach

Let us now present a few simulated Stokes V dynamic spectra to illustrate the argument of the previous section. In each following simulation, the magnetic field is assumed to be equal to zero everywhere, except in a circular spot located at phase 0.5, covering 2% of the total stellar surface and in which the field strength is 500 G and the filling factor is 1. The *orientation* of field lines (assumed constant inside the spot) as well as the spot latitude vary from one simulation to the next. Additionally, we consider the case of both high and low stellar inclination angles (the line-of-sight projected rotational velocity $v \sin i$ being set to 40 km s^{-1}). Calculating the Stokes V dynamic signatures of these elementary field distributions amounts to computing the columns of the response matrix associated to the corresponding image pixels. Note that such field configurations are nothing but test cases, with no claim to represent some kind of real field topology. Some of them even transgress basic physical laws (Maxwell's equations are violated at both east and west boundaries of a purely azimuthal field feature for instance) but they remain nevertheless very convenient images for the kind of testing we wish to perform.

We first consider a star with an inclination angle $i = 30°$. In Fig. 1, we show the dynamic Stokes V spectra corresponding to a low latitude (left panels) and high latitude (right panels) spot, and for all three field components (top to bottom). We can first check that the amplitude modulation of the Zeeman signature generated by an azimuthal field structure (bottom row) is indeed antisymmetric around $\phi = 0.5$ (the number of grey levels *right* to the dashed line at phase $0.5 - \phi$ is the same as that *left* to the dashed line at phase $0.5 + \phi$). In contrast, Zeeman signatures from radial and meridional features (two upper rows) are *symmetrically* modulated in amplitude around $\phi = 0.5$. Note that some departures from strict symmetry (or antisymmetry) can be observed locally due to the fact that the field is not localised in a single pixel (as assumed for the analytical approach of Sect. 2.2), but spreads out over an extended region covering about 2% of the total stellar surface.

While Zeeman signatures from azimuthal and radial/meridional field spots are obviously different, those from low latitude radial and meridional field regions are very similar. A closer look to the corresponding dynamic spectra reveals some departures though, with a Stokes V signal from a low latitude meridional field spot extending to higher and lower phases than its radial field counterpart for instance. However, differences are very subtle and will surely be hard to retrieve from data sets, especially when phase sampling is sparse (as often the case in real world). Note that both signatures have approximately the same overall size, indicating that inversion crosstalk between radial and meridional field components will occur in both directions. The situation changes drastically for high latitude (circumpolar) features whose Zeeman signatures can now be followed

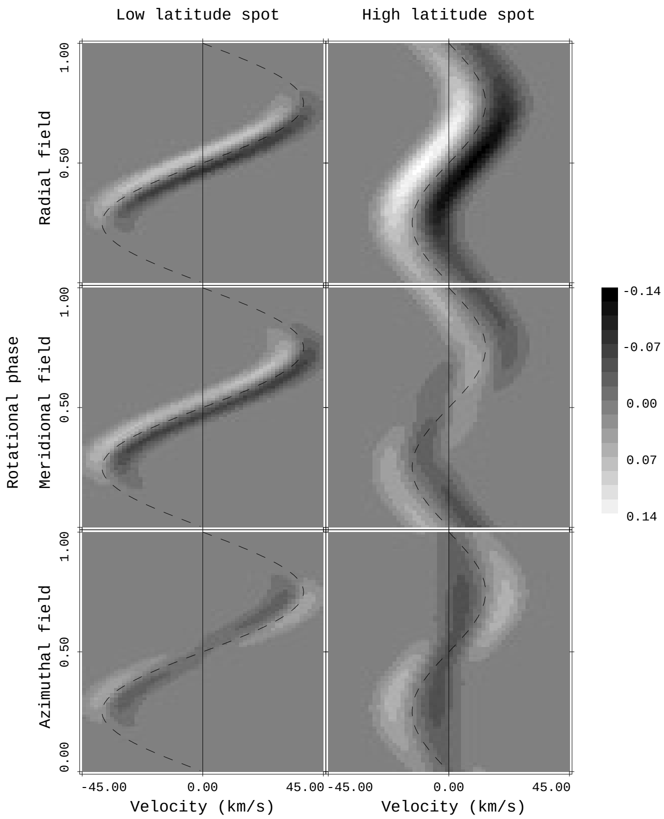

Fig. 1. Dynamic Stokes V spectra for an elementary field geometry consisting of a single circular spot (centred on phase 0.5) inside which the field strength is 500 G. Each line of each dynamic spectrum is a circular polarisation signature coded with the grey scale lookup table shown on the right (and labelled in% of the continuum level). From top to bottom, the field orientation inside the spot is successively radial (top row), meridional (middle row) and azimuthal (bottom row). The spot latitude is either 20° for the left panels, and 70° for the right ones. The assumed stellar inclination angle i is 30°. The full vertical line in each graph indicates the line centre while the dashed sinusoid depicts the radial velocity excursion of the spot centre throughout a full rotational cycle

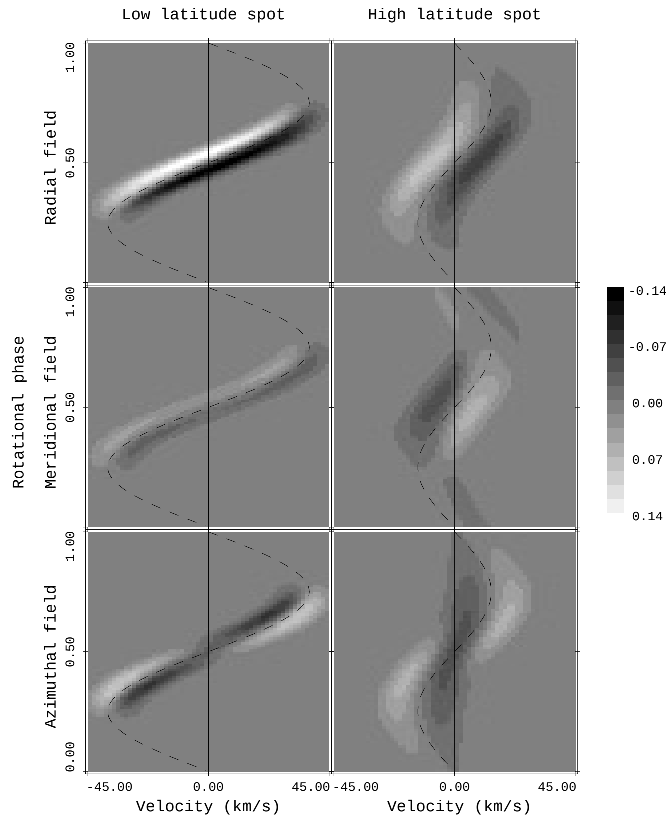

Fig. 2. Same as Fig. 1 for a stellar inclination angle of i = 60°

throughout a much larger phase span (a whole rotation cycle). In particular, we now have access to sufficient information to enable clear identification of the parent field orientation.

Fig. 2 presents the case of a star with an axial inclination of 60°. The overall situation is similar to the previous one (symmetric and antisymmetric Stokes V signatures for radial/meridional and azimuthal field features respectively), except for the following point. Although Stokes V signatures from low latitude radial and meridional field features are still somewhat similar in shape (though not as much as in Fig. 1), their respective intensity are now radically different. We thus expect ZDI to be very weakly sensitive to low latitude meridional features (such fields are indeed almost always perpendicular to the line of sight for a roughly equator-on star). This low amplitude signature should then be reconstructed as a weak *radial* field, according to the conclusions obtained in the previous section.

As a conclusion to this section, we can say that dynamic spectra are useful tools to characterise the magnetic orientation of field vectors on rapidly rotating objects. One important difference is that radial and meridional fields generate symmetric Zeeman signatures, while azimuthal field introduces some asymmetry in these signatures (see Fig. 3), the asymptotic situation (i.e. antisymmetry) corresponding to a purely azimuthal field.

4. Maximum entropy inversion

4.1. Reconstruction in optimal conditions

In this section, we present results of a full maximum entropy reconstruction of a complex magnetic test distribution, for various values of the axial inclination. The influence of a few important instrumental limitations (finite S/N ratio and limited phase coverage) are also discussed. The selected test distribution features six circular spots that together cover 12% of the total stellar surface, and in which the field strength is 500 G (with unit filling factor). Half the spots (one per field orientation) are located at low latitude (20°), the others being circumpolar (at a latitude of 70°). The line-of-sight projected rotational velocity $v \sin i$ is set to 40 km s^{-1}. The line profile model is that described in Sect. 2 and will be further discussed in Sect. 4.3.

In the first simulation (see Fig. 4), we use a stellar axial inclination i of 30°. The corresponding synthetic data set in-

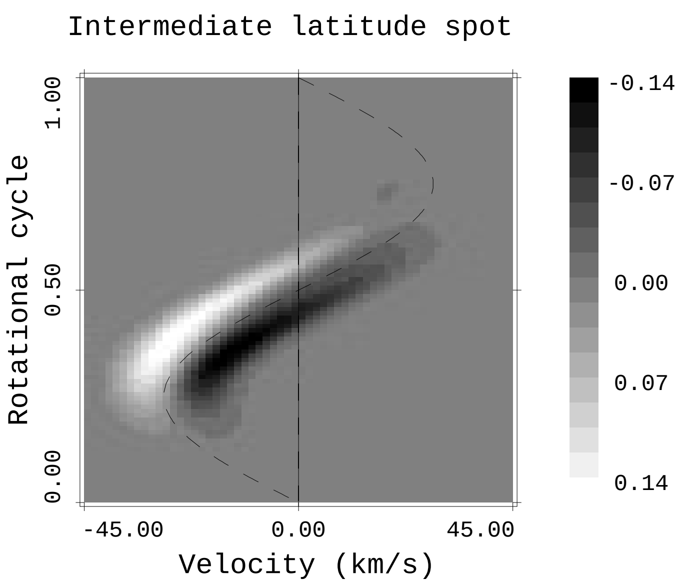

Fig. 3. Dynamic spectrum for a 500 G radial plus 500 G azimuthal field spot at intermediate latitude (45°), for an axial inclination of 60°. The associated Zeeman signature is clearly asymmetric (more intense in the blue part of the line than in the red), witnessing the presence of an azimuthal field

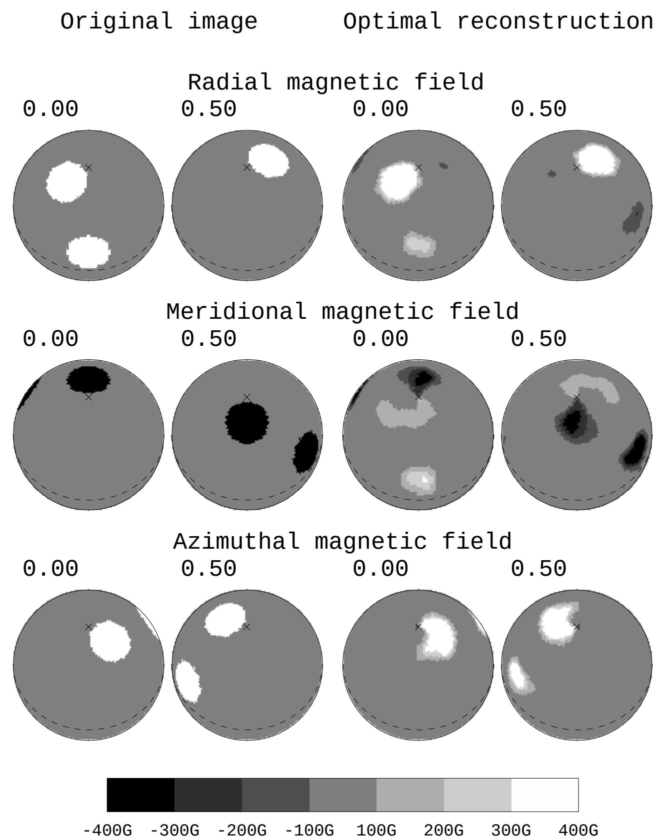

Fig. 4. Six spot star simulation for an axial inclination i = 30°. The corresponding data set includes Stokes V profiles computed at 10 evenly spaced phases, and noised at a relative level of 2×10^{-5}. The original and reconstructed images (two first and two last columns respectively) are shown at phases 0.0 and 0.5, for each field component (top to bottom)

cludes Stokes V profiles computed at 10 evenly spaced phases. The reconstructed distribution corresponds to a unit reduced χ^2 maximum entropy fit to the synthetic data, with noise at a relative level of 2×10^{-5} (i.e. S/N = $50,000$) per 3 km s^{-1} spectral bin. Although incredibly low, such relative noise levels can nevertheless be obtained on very bright objects with cross-correlation techniques (e.g. Least-Squares Deconvolution, Donati et al. 1997). As predicted in the previous two sections, the code is quite successful in distinguishing azimuthal field regions from radial/meridional field ones. For low latitude radial/meridional field features, a very clear crosstalk is observed, mainly from the radial to the meridional field component. Note in particular that the low latitude radial field spot is reconstructed as a predominantly meridional field feature. We therefore conclude that there is significant ambiguity for reconstructed low latitude radial/meridional field features as whether their parent field is actually radial or meridional. On the other hand, only little crosstalk is observed for high latitude spots, whose parent field direction can thus be properly identified.

The second simulation (see Fig. 5) is exactly the same as the first one, except for the stellar axial inclination, now set to 60°. Once more, the code clearly distinguishes radial/meridional from azimuthal field features. As expected from such a stellar orientation, Stokes V signatures are very weakly sensitive to low latitude meridional field features (which are almost always perpendicular to the line of sight). The low amplitude residual polarisation signature is reconstructed as a weak radial field according to the predictions of Sect. 2. Concerning the low latitude radial field spot, the conclusion is different than in the previous example; since ZDI is so weakly sensitive to low latitude meridional field features, we can conclude that the most probable field inclination for the reconstructed field feature is *radial* (as a meridionally oriented field would indeed need to be five to ten times more intense to generate the same Stokes V signature, thus implying an unreasonably strong magnetic flux). For high latitude (circumpolar) features, the code has no problem reconstructing the orientation of the parent magnetic field.

One important conclusion of this section is that increasing the number of spots does not "wash out" the Stokes V signal of individual regions and that conclusions obtained for single spot distributions apply with no major modification to complex multiple spot topologies.

4.2. Effects of photon noise and poor rotational phase sampling

Fig. 6 shows new reconstructions of the original test image of Fig. 4 (i = 30°), now from synthetic data with noise at relative levels of 5×10^{-5} (i.e. S/N = $20,000$) and 1.25×10^{-4} (i.e. S/N = $8,000$) per 3 km s^{-1} spectral bin. This is typical to what ZDI can achieve on most objects observed to date, independently of rotation rate and up to a V magnitude of about 9 (see Donati et al. 1997). In particular, we see that very similar results

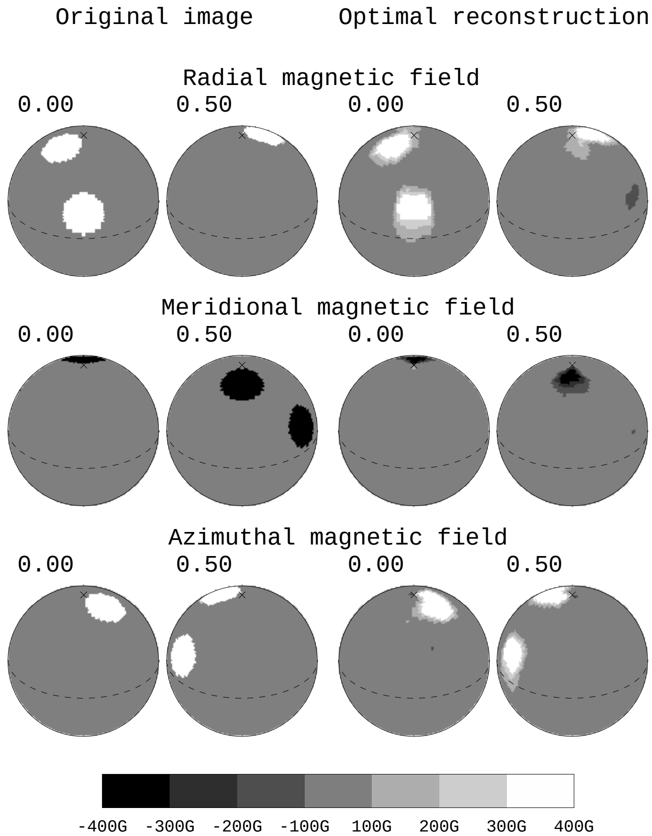

Fig. 5. Same as Fig. 4 for an axial inclination of i = 60°

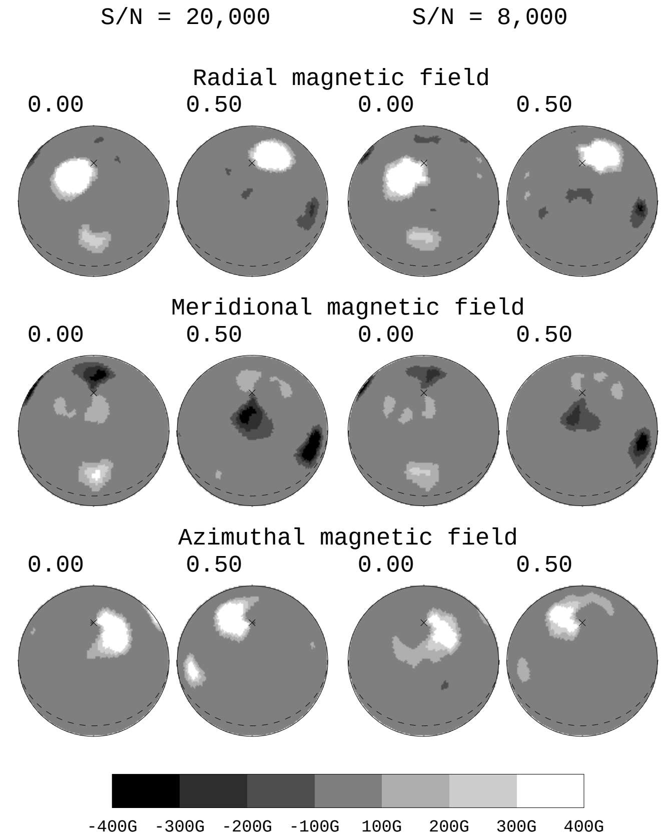

Fig. 6. Simulation of Fig. 4, with a relative noise in the Stokes V profiles increased to a level of 5×10^{-5} (i.e. S/N = 20, 000, left two columns), and to a level of 1.25×10^{-4} (i.e. S/N = 8, 000, right two columns)

(compared to the optimal reconstruction of Fig. 4) are obtained at S/N = 20, 000, while some features start to vanish (and especially the low latitude azimuthal field region and the high latitude meridional field one) when S/N drops down to 8,000. At S/N = 3, 200 (no corresponding figure shown), no more than the high latitude radial field feature and a very dimmed version of the high latitude azimuthal field region are visible in the maximum entropy image; it therefore sets a rough lower limit in S/N of about 5,000 for ZDI to reconstruct most magnetic features present in the original field distribution. Note however that this threshold strongly depends on the assumed local magnetic flux at the surface of the star to be imaged (set to 500 G in the present simulation) as well as on other observational parameters like for instance the total number of rotational phases at which the star was monitored (10 in this particular example) or the strength and magnetic sensitivity of the "average" local line profile (see Sect. 2.1).

Similarly, Fig. 7 (left two columns) features the reconstruction of the same image, from a data set sampled at only three evenly spaced phases (0.17, 0.50 and 0.83) and with the original relative noise level of 2.0×10^{-5}. We observe once more that some features have almost completely disappeared (mainly the high latitude meridional and azimuthal field spots). Crosstalk problems (for the low latitude meridional field feature for instance) are also slightly enhanced. For both cases, it is important to note that decreasing data quality (either in S/N ratio or in phase sampling) results in no more than losing a certain number of spots, but introduces *no spurious features* in the reconstructed image.

On the left two columns of Fig. 7, the original image of Fig. 4 is reconstructed from a data set sampled at three groups of phase pairs (0.17 & 0.22, 0.50 & 0.55, 0.83 & 0.88). Although the overall phase coverage is still rather poor (with three large phase gaps as in the first simulation of Fig. 7), the quality of the recovered image is considerably better, with all original features now reconstructed reasonably well. It is important to understand that this improvement does not just come from doubling the number of phases (and therefore the total number of collected photons), but rather from the fact that *short time sampling* (on typical timescales of a few% of a rotational cycle) also contains very rich information for magnetic imaging. This is particularly interesting for stars like HR 1099 for which the rotational period is close to a small integer number of days, and for which very useful data sets can still be collected even within a limited number of nights.

4.3. Errors on atmospheric parameters and local line profile modelling

As demonstrated in Donati & Cameron (1997), one can easily derive a relatively accurate estimate for both "average" intrinsic line profile (from Least-Squares Deconvolution of slowly rotating standard stars with similar spectral types) and stellar atmospheric parameters of interest for imaging (from iterative maximum entropy reconstructions). However, it is still interesting to know the kind of impact possible spectral modelling errors can have on the reconstruction process, to determine in particular to what accuracy level these parameters must be obtained.

An important point to recall first is that the background level (i.e. the blank star profile) on which polarisation signatures add up is perfectly known for ZDI ($\mathbf{B} = 0$ implies $V = 0$). Therefore, unlike conventional Doppler imaging for which wrong spectral atmospheric parameters (and in particular small errors in $v \sin i$ and/or in the continuum limb darkening constant) can generate longitude independent artifacts in the derived brightness map (Vogt et al. 1987), ZDI should be free of such zero-order pollution of the reconstructed magnetic image. We indeed observe from simulations that errors of up to 10% in $v \sin i$ (i.e. at least twice larger than typical errors on this parameter for moderate to fast rotators) produce for instance nothing more than small latitude shifts of low latitude magnetic features (as well as a weak increase of the average rms level to which the data can be fitted) but do not generate any kind of ring-like artifacts as in conventional Doppler imaging.

A second step consists in looking to what extent the use of an incorrect local line profile model (when fitting the observed Zeeman signatures) can generate artifacts in the reconstructed magnetic map (e.g. Unruh & Cameron 1995). The very simple test we carried out consists in performing a maximum entropy fit to the original data set of Fig. 4, with an intrinsic line profile (called “model profile” in the following) that differs from that used to generate the input spectra (called “original profile”). Although we still assume that this model intrinsic profile is Gaussian, we distort it both in overall strength and width with respect to the original local profile.

Increasing the *intensity* of the model profile trivially results in globally expanding the Stokes V derivatives of the response matrix (as already discussed in Sect. 2.1), and thus in scaling down the recovered magnetic distribution as a whole. Decreasing the *width* of the model intrinsic profile (by 50% or more) or increasing it moderately (by up to about 25%) introduces almost no change in the derived maximum entropy image (reconstructed features getting only slightly larger or smaller respectively, to compensate for the error in profile width). Broadening the model intrinsic profile still further progressively degrades the optimal quality of the fit to the data, with a final rms accuracy rising from 2×10^{-5} to about 10^{-4} for a 50% increase in local profile width. Even with such a large amount of excess broadening in the model intrinsic profile, the impact on the reconstructed magnetic image is only moderate, consisting essentially in weak small-scale artifacts popping up in the magnetic image (in the radial field map mainly). These artifacts correspond to the only solution the code is left with for artificially sharpening the reconstructed Stokes V signatures, once the reconstructed magnetic features have been reduced to the smallest possible size (given the observed rotational modulation). Note that, at noise levels ZDI can typically achieve for most objects observed to date (i.e. $0.5 - 2.0 \times 10^{-4}$), these artifacts are almost undistinguishable from others already present in the image and due for instance to low-level crosstalk between field components (see Fig. 6) or poor rotational coverage (see Fig. 7).

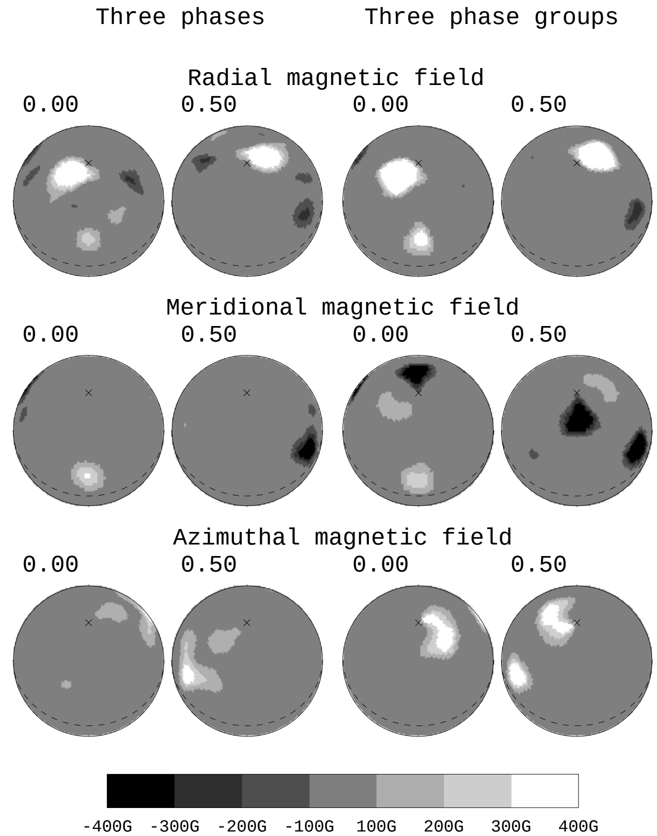

Fig. 7. Simulation of Fig. 4, with a poor Stokes V profile sampling. The left image is recovered from a even three phase data set, while the right one is reconstructed from three evenly spaced groups of phase pairs (see text)

As determining the width of the mean intrinsic line profile to better than 20–50% is easy (e.g. Donati & Cameron 1997), we can thus conclude that a perfect knowledge of the spectral model is definitely not a major constraint for ZDI (as it is for conventional Doppler imaging, Unruh & Cameron 1995), but rather no more than a standard calibration problem. In particular, it does not modify the above conclusions about the sensitivity of ZDI to field orientation.

5. Conclusions

In this paper, we have presented three different complementary approaches to study the sensitivity of ZDI (from circular spectropolarimetric observations alone) to orientations of magnetic field vectors. While the analytical approach can be used for sensitivity predictions, the forward approach helps studying in detail the true response of ZDI and can give some useful direct and immediate diagnosis about the local field orientation at the surface of rapidly rotating stars. Finally, the full maximum entropy inversion validates all conclusions and helps determining the optimal observing conditions.

We conclude that ZDI is always very good at distinguishing azimuthal from radial/meridional field features. For high latitude (circumpolar) magnetic regions, we can even reliably recover the original radial and meridional field subcomponents. For low latitude (non circumpolar) features however, we observe that ZDI is prone to crosstalk between radial and meridional field components (from radial to meridional field mainly at low inclination angles, and the opposite for high inclination angles). This crosstalk is most severe for pole-on stars (for which any diagnosis about the original orientation of a recovered low latitude radial/meridional field vector becomes hazardous). We also note that the sensitivity of ZDI to low latitude meridional field vectors decreases significantly as stellar inclination increases (those fields being almost always perpendicular to the line of sight at high inclination angles).

Degrading the data quality (either in S/N ratio or phase coverage) does not modify these conclusions significantly, the main effect being nothing more than rubbing out of the reconstructed magnetic topology some of the original field features (those with either weakest Stokes V signatures and/or lowest visibility). An interesting characteristic of magnetic imaging is that short time rotational modulation of Stokes V signatures can partly compensate from poor overall phase coverage. Finally, we observe that, although a good knowledge of stellar atmospheric parameters and local intrinsic profile provides a better calibration of the image, it is definitely not as crucial a problem as in conventional Doppler imaging and does not modify the above conclusions about the sensitivity of ZDI to field orientation.

ZDI therefore represents an optimal tool for investigating stellar dynamo modes, and observing in particular the long term (cyclic?) evolution of the toroidal and poloidal component of the associated magnetic topology. The obvious advantage of ZDI on the other (yet untested) magnetic imaging method proposed by Saar et al. (1992, 1994) – aiming at reconstructing magnetic maps from rotational modulation of magnetically broadened and intensified spectral lines observed in unpolarised light – is of course its sensitivity to the *vector properties* of the field. Optimally, one would of course like to apply a generalised version of ZDI to both polarised and unpolarised *infrared* échelle spectra, where the relative Zeeman sensitivity of spectral lines is considerably higher (see for instance Saar 1996). In particular, such an improvement should in principle yield simultaneous reconstructions of both local magnetic field vector and filling factor. However, the corresponding instruments and detectors (e.g. IRTF/CSHELL, NOAO/PHOENIX) are still rare and less competitive (both in throughput and overall wavelength coverage) than their visible equivalents (at present time) nor are they equipped with adequate polarimetric facilities.

A more obvious and immediate progress may come from the addition of linear spectropolarimetry to the inversion process. With the new visitor AAT/UCLES polarimeter presently in construction in Meudon, or with the MuSiCoS spectrograph dedicated polarimetric module (both equipped for linear polarimetry), we should soon know whether Stokes Q and U signatures in line profiles are detectable in cool active stars. In case so, we will be able to constrain further and determine more accurately the magnetic field topologies of such objects.

Acknowledgements. JFD acknowledges IAU for travel funds and CNRS for living expenses that enabled him to present some of these results at IAU Symp. 176 on “Stellar Surface Structures”. SFB is grateful for an Australia-France COoperation Program (AFCOP) grant and a French Government Scientific Fellowship that enabled him to spend 4 months working at Meudon. We also thank the referees, Artie Hatzes and Steven Saar, for suggesting several modifications for improving and clarifying the paper.

References

Baliunas S.L., Donahue R.A., Soon W.H., et al., 1995, ApJ 438, 269
Brandenburg A., Tuominen I., 1992, in: Tuominen I., Moss D., Rüdiger G. (eds.), IAU Coll. 130, “The Sun and Cool Stars: Activity, Magnetism, Dynamos”. Springer, Berlin, p. 223
Brown S.F., Donati J.-F., Rees D.E., Semel M., 1991, A&A 250, 463
Donati J.-F., Brown S.F., Semel M. et al., 1992, A&A 265, 682
Donati J.-F., Cameron A.C., 1997, MNRAS (in press)
Donati J.-F., Semel M., Carter B.D., Rees D.E., Cameron A.C., 1997, MNRAS (submitted)
Semel M., 1989, A&A 225, 456
Saar S.H., Piskunov N.E., Tuominen I., 1992, in: Giampapa M.S., Bookbinder J. (eds.), 7th Cambridge Workshop on Cool Stars, Stellar Systems and the Sun. ASP Conf. Series 26, p. 255
Saar S.H., Piskunov N.E., Tuominen I., 1994, in: Caillault J.-P. (ed.), 8th Cambridge Workshop on Cool Stars, Stellar Systems and the Sun. ASP Conf. Series 64, p. 661
Saar S.H., 1996, in: Strassmeier K.G., Linsky J.L. (eds.), IAU Symp. 176, “Stellar Surface Structure”. Kluwer Academic Publishers, Dordrecht, p. 237
Unruh Y.C., Cameron A.C., 1995, MNRAS 273, 1
Vogt S.S., Penrod G.D., Hatzes A.P., 1987, ApJ 321, 496

This article was processed by the author using Springer-Verlag LaTeX A&A style file *L-AA* version 3.